Enhanced magnetic moment in ultrathin Fe-doped $CoFe_2O_4$ films

J. A. Moyer,[1,*] C. A. F. Vaz,[2] D. P. Kumah,[1] D. A. Arena,[3] and V. E. Henrich[1]

[1]*Department of Applied Physics and Center for Research on Interface Structures and Phenomena, Yale University, New Haven, Connecticut 06511, USA*

[2]*SwissFEL, Paul Scherrer Institut, 5232 Villigen PSI, Switzerland*

[3]*National Synchrotron Light Source, Brookhaven National Laboratory, Upton, New York 11973, USA*

(Received 3 August 2012; revised manuscript received 10 October 2012; published 5 November 2012)

The effect of film thickness on the magnetic properties of ultrathin Fe-doped cobalt ferrite ($Co_{1-x}Fe_{2+x}O_4$) grown on MgO (001) substrates is investigated by superconducting quantum interference device magnetometry and x-ray magnetic linear dichroism, while the distribution of the Co^{2+} cations between the octahedral and tetrahedral lattice sites is studied with x-ray absorption spectroscopy. For films thinner than 10 nm, there is a large enhancement of the magnetic moment; conversely, the remanent magnetization and coercive fields both decrease, while the magnetic spin axes of all the cations become less aligned with the [001] crystal direction. In particular, at 300 K the coercive fields of the thinnest films vanish. The spectroscopy data show that no changes occur in the cation distribution as a function of film thickness, ruling this out as the origin of the enhanced magnetic moment. However, the magnetic measurements all support the possibility that these ultrathin Fe-doped $CoFe_2O_4$ films are transitioning into a superparamagnetic state, as has been seen in ultrathin Fe_3O_4. A weakening of the magnetic interactions at the antiphase boundaries, leading to magnetically independent domains within the film, could explain the enhanced magnetic moment in ultrathin Fe-doped $CoFe_2O_4$ and the onset of superparamagnetism at room temperature.

DOI: 10.1103/PhysRevB.86.174404 PACS number(s): 75.70.Ak, 75.30.−m, 75.50.Gg, 75.20.−g

I. INTRODUCTION

Magnetic oxides have garnered much attention recently for their potential use in spintronic devices, where the spin of the electron is utilized along with the charge to design devices with novel functionalities.[1–3] In particular, 3*d* transition-metal magnetic oxides can exhibit a wide variety of magnetic behavior, owing to their highly correlated *d* electrons.[4] A reduction in thickness of metal oxide thin films can result in significant changes in the magnetic properties, as demonstrated in the phase transition of $La_{0.7}Sr_{0.3}MnO_3$ from a ferromagnetic conductor to a nonmagnetic insulator below a critical thickness of ∼1.2 nm.[5] Multiple ultrathin 3*d* transition-metal spinel ferrites (i.e., Fe_3O_4,[6] $CoFe_2O_4$,[7] and $NiFe_2O_4$[8]) have also been shown to have magnetic moments that change with film thickness; however, unlike $La_{0.7}Sr_{0.3}MnO_3$, their magnetic moments increase for thicknesses below ∼10 nm. In Fe_3O_4 this enhanced magnetic moment has been attributed to an observed phase transition to a superparamagnetic state,[6] while in $CoFe_2O_4$ and $NiFe_2O_4$ this enhanced magnetic moment has been suggested to be caused by a change in the distribution of cations between the octahedral and tetrahedral lattice sites.[7,8]

The 3*d* transition-metal spinel ferrites MFe_2O_4 ($M = 3d$ transition-metal cation) have the spinel crystal structure, in which 2/3 of the cations are octahedrally coordinated and 1/3 of the cations are tetrahedrally coordinated. They are classified as either normal or inverse depending on whether the divalent cations occupy tetrahedral or octahedral sites, respectively. The crystal structure is often a mix between these two structures and can be quantified by an inversion parameter λ, which is defined as the fraction of divalent cations that reside on the octahedral sites ($\lambda = 0$ for normal, 1 for inverse). Spinel ferrites have received much attention for use in spintronics applications due to their large predicted spin polarizations and their high magnetic critical temperatures (T_c), typically well above room temperature.[9–13] They have been successfully incorporated into a number of spintronics devices, such as $Fe_3O_4/CoCr_2O_4/La_{1-x}Sr_xMnO_3$ magnetic tunnel junctions,[14] $CoFe_2O_4$[15] and $NiFe_2O_4$[16] spin filters, and $CoFe_2O_4/BaTiO_3$ multiferroic nanostructures.[17] In addition, Fe doping ($M_{1-x}Fe_{2+x}O_4$) has been shown to alter the magnetic moments of $Co_{1-x}Fe_{2+x}O_4$[18] and $Zn_{1-x}Fe_{2+x}O_4$[19] in a nonlinear manner as the Fe doping level changes, and to drastically decrease the resistivity of many of the insulating 3*d* spinel ferrites.[19–22]

In this study the effect of film thickness on the magnetic properties of Fe-doped $CoFe_2O_4$ ($Co_{1-x}Fe_{2+x}O_4$) is investigated to determine whether superparamagnetism or a change in the cation distribution is the underlying cause for the enhanced magnetic moment in these ultrathin ferrite films. The bulk magnetic properties are measured with superconducting quantum interference device (SQUID) magnetometry, and the cation specific magnetic properties are determined with x-ray magnetic linear dichroism (XMLD). In addition, this work directly measures the cation distribution in Fe-doped $CoFe_2O_4$ films using x-ray absorption spectroscopy (XAS) and ligand field multiplet (LFM) calculations to determine if a decrease in film thickness has an effect on the inversion parameter of Fe-doped $CoFe_2O_4$, as has been hypothesized in the case of $CoFe_2O_4$[7] and $NiFe_2O_4$.[8] We find that, with a reduction in film thickness, the magnetic moment increases for all $Co_{1-x}Fe_{2+x}O_4$ films with Fe doping levels of $0 \leqslant x \leqslant 0.78$; however, there is no significant change in the inversion parameter as a function of film thickness for any of the stoichiometries, eliminating a change in the cation distribution as a possible cause for this enhanced magnetic moment. Furthermore, the SQUID and XMLD data support the conclusion that the films are transitioning into a superparamagnetic state in the ultrathin regime, and that this is responsible for the enhanced magnetic moment seen in these ultrathin ferrite films.

A short review of the unique magnetic properties of thin-film $CoFe_2O_4$ and Fe-doped $CoFe_2O_4$ is helpful before investigating the effects of reducing the film thickness. $CoFe_2O_4$ has a partially inverse spinel crystal structure with the Co^{2+} cations predominantly occupying the octahedral sites. It has a measured inversion parameter ranging from 0.76 to 0.98;[23,24] as Fe is doped into $CoFe_2O_4$, Fe^{2+} cations only occupy octahedral sites, resulting in an increase of the inversion parameter towards a fully inverse spinel crystal structure for Fe_3O_4.[20,25] The octahedral and tetrahedral sites are aligned antiferromagnetically, resulting in a ferrimagnet that has a bulk T_c of 793 K for $CoFe_2O_4$ and 858 K for Fe_3O_4.[13] The bulk magnetic moment of $CoFe_2O_4$ is 3.7 μ_B/formula unit (f.u.); however when thin films are grown on substrates that have a higher symmetry, such as MgO and $SrTiO_3$, the magnetic moment is reduced to 25–60% of its bulk value.[7,18,26–28] Upon Fe doping, the magnetic moment tends closer to its bulk value as the Fe doping level is increased, leading to a magnetic moment for an Fe_3O_4 thin film that is reduced from its bulk value by only a few percent.[18] This reduction in magnetic moment has been seen in several ferrites and has been attributed to strain, a partially inverse spinel crystal structure, and/or antiphase boundaries, which form when islands that nucleate at different areas of the substrate merge and are out of phase with each other.[18,29] $CoFe_2O_4$ and Fe-doped $CoFe_2O_4$ are unique among the ferrites in that they have a large magnetic anisotropy, which is due to a spin-orbit stabilized ground state and unquenched orbital momentum, caused by a trigonal crystal field on the Co^{2+} cations.[4,26,30–34] This results in $CoFe_2O_4$ having a cubic magnetocrystalline anisotropy constant K_1 that is over an order of magnitude larger and of opposite sign than the other stoichiometric spinel ferrites.[13] These unique magnetic properties have resulted in $CoFe_2O_4$ being used extensively as magnetic spin filters[15,35] and in strain-driven multiferroic nanostructures.[17,36–39] In addition, the magnetic properties exhibited by Fe-doped $CoFe_2O_4$ present the possibility of using it in other spintronic devices, such as charge-driven multiferroic heterostructures.

II. EXPERIMENTAL DETAILS

Thin films of $Co_{1-x}Fe_{2+x}O_4$ (001) were grown epitaxially on MgO (001) substrates by oxide molecular beam epitaxy (oxide-MBE) with nominal stoichiometries of $x = 0$, 0.19, 0.60, and 0.78 (actual stoichiometries were measured with *in situ* x-ray photoelectron spectroscopy immediately following film growth and have a standard deviation of 0.03 from their nominal values). For each stoichiometry, films with thicknesses of 3.4, 6.7, 10.1, 13.4, and 20.0 nm were grown, except that there was no 20 nm film for $x = 0.78$. The lattice mismatch between the oxygen sublattices of $Co_{1-x}Fe_{2+x}O_4$ and MgO is very small (−0.4%), permitting cube-on-cube epitaxial growth of $Co_{1-x}Fe_{2+x}O_4$. The growth conditions and structural properties for the 20.0 nm films have previously been published;[20] the same growth conditions were used to grow the thinner films, resulting in structural properties that are nearly identical to the 20.0 nm films, as measured with reflection high energy (RHEED) and low energy (LEED) electron diffractions. The growth rate was calibrated with a quartz crystal thickness monitor, and film thicknesses were confirmed with x-ray reflectivity measurements. Before removal from the growth chamber, all samples were capped with 1 nm of MgO to prevent surface oxidation.[20]

Bulk magnetic properties were measured using a SQUID magnetometer (Quantum Design MPMS), while cation-specific magnetic properties were measured with XMLD. The cation distribution for each sample was determined from XAS. The XAS and XMLD measurements were performed on beamline U4B at the National Synchrotron Light Source (spectra measured in total electron yield mode with an energy resolution of ∼0.34 eV). The linear dichroism was measured with the samples in a remanent magnetized state in the out-of-plane direction and rotated with respect to the x-ray beam. All measurements were performed at 300 K, except for the SQUID measurements, which were also performed at 100 K.

III. RESULTS

A. Magnetic properties

The effect of film thickness on the magnetic properties of ultrathin $Co_{1-x}Fe_{2+x}O_4$ is determined by measuring the magnetic response of each sample using a SQUID magnetometer. The magnetic field was aligned along either the [010] or [001] crystal direction to measure the in-plane or out-of-plane magnetic properties, respectively. In-plane and out-of-plane M-H loops measured at 100 K for samples with Fe doping levels of $x = 0$, 0.19, 0.60, and 0.78 and thickness of 3.4 to 20.0 nm are displayed in Fig. 1; a diamagnetic contribution, similar for all samples, was removed from each M-H loop. The shapes of the M-H loops for the 10.1, 13.4, and 20.0 nm films are all similar to each other; however, as the film thickness decreases to 6.7 and 3.4 nm, the shapes of the loops begin to change. These thinner films exhibit a large increase in saturation magnetic moments and a decrease in coercive fields.

It has previously been determined that the easy axis of the 20.0 nm samples is out-of-plane;[18] however, as the film thickness is reduced, it is not clear whether the easy axis is in-plane or out-of-plane. From the M-H loops in Fig. 1, it is clear that the coercive fields for nearly all the samples are much larger in the out-of-plane direction than the in-plane direction (the only samples in which this is not true are the 3.4, 6.7, and 13.4 nm $CoFe_2O_4$ films, where the large measurement noise may introduce some error in determining the coercive fields). However, the magnetic moments do not behave in a similar manner. To better understand how the magnetic moments are changing with film thickness, Fig. 2 plots the in-plane and out-of-plane saturation and remanent magnetic moments as a function of film thickness; the dotted lines are the bulk magnetic moments for each stoichiometry, assuming a full ferrimagnetic alignment between the octahedral and tetrahedral sites.[13] The in-plane and out-of-plane saturation magnetic moments are roughly equal for the films with thickness between 10.1 and 20.0 nm, but as the film thickness is reduced to 6.7 and 3.4 nm, the in-plane saturation magnetic moments become much larger compared to the out-of-plane magnetic moments (this is not seen in the 6.7 nm $CoFe_2O_4$ film, possibly due to the measurement noise mentioned above). Conversely, the remanent magnetizations are generally larger in the out-of-plane direction than the in-plane direction for all

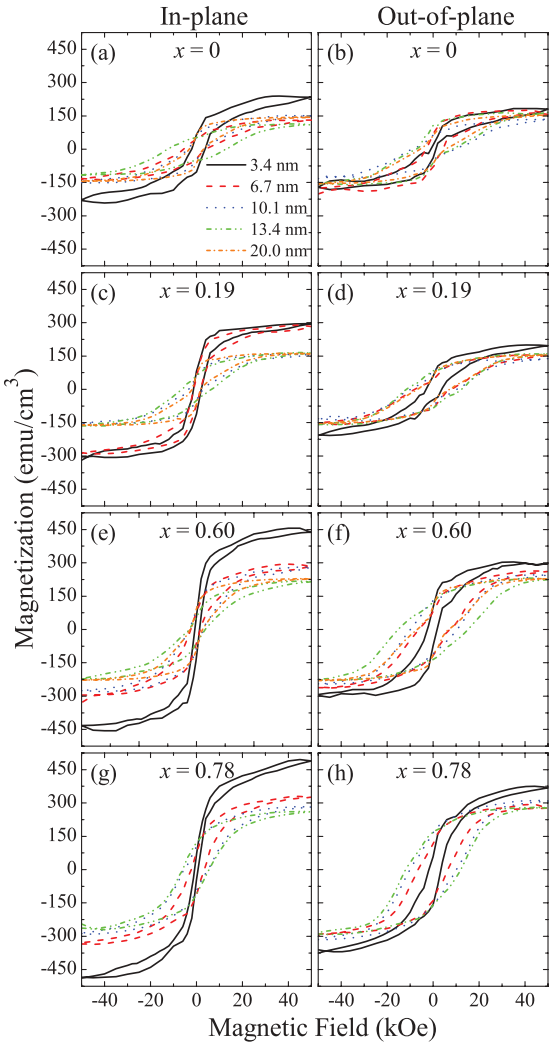

FIG. 1. (Color online) In-plane and out-of-plane M-H loops at 100 K of $Co_{1-x}Fe_{2+x}O_4$ films with stoichiometries of (a) and (b) $x = 0$, (c) and (d) $x = 0.19$, (e) and (f) $x = 0.60$, and (g) and (h) $x = 0.78$, respectively.

stoichiometries at all thickness, with this effect enhanced for the $x = 0.60$ and $x = 0.78$ samples. The larger coercive fields and remanent magnetic moments in the out-of-plane direction compared to the in-plane direction lead to the conclusion that the magnetic easy axis is out-of-plane for all samples, even with the surprising behavior of the saturation magnetic moments of the thinnest samples being larger in the in-plane direction than in the out-of-plane direction. It is important to note that the magnetic moments never increase to above their bulk values, which was reported for $CoFe_2O_4/SrTiO_3$.[7]

Out-of-plane M-H loops taken at 300 K, shown in Figs. 3(a)–3(d) for samples with nominal stoichiometries of $x = 0.00$, 0.19, 0.60, and 0.78, respectively, demonstrate how temperatue affects the magnetic properties of the films. Compared with the M-H loops at 100 K, the saturation and remanent magnetizations and coercive fields are much reduced for all samples. However, while the saturation magnetizations at 300 K decrease to ∼90% of their 100 K values, the remanent magnetizations decrease dramatically to ∼18% of their 100 K values for the thinnest films (3.4 and 6.7 nm). As

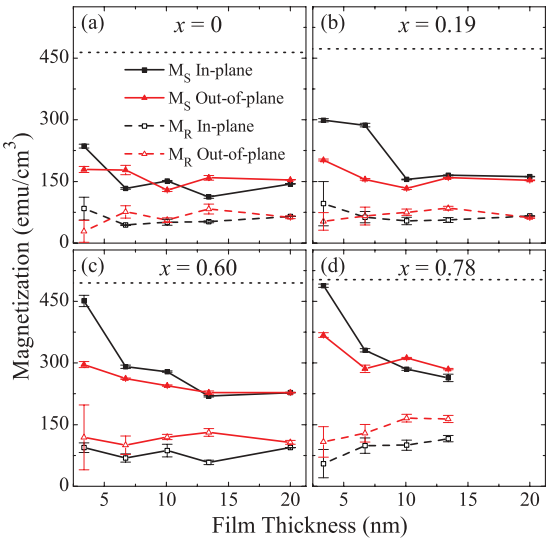

FIG. 2. (Color online) In-plane and out-of-plane saturation and remanent magnetic moments vs film thickness for $Co_{1-x}Fe_{2+x}O_4$ films with stoichiometries of (a) $x = 0$, (b) $x = 0.19$, (c) $x = 0.60$, and (d) $x = 0.78$ measured at 100 K. The dotted lines correspond to the bulk magnetic moment for each stoichiometry.

the film thickness increases, this decrease in the remanent magnetization lessens to ∼25%, 30%, and 38% for film thickness of 10.1, 13.4, and 20.0 nm, respectively. This strong decrease seen in the remanent magnetization as the temperature is increased to 300 K is mirrored by the coercive fields, which decrease to ∼11% of their 100 K values for the thinnest films (3.4 and 6.7 nm), before lessening to ∼19% as the thickness is increased to 20 nm. This near vanishing of the coercive fields and remanent magnetic moments in the thinnest films is evidence that there is a sharp reduction of the magnetic anisotropy in these films.

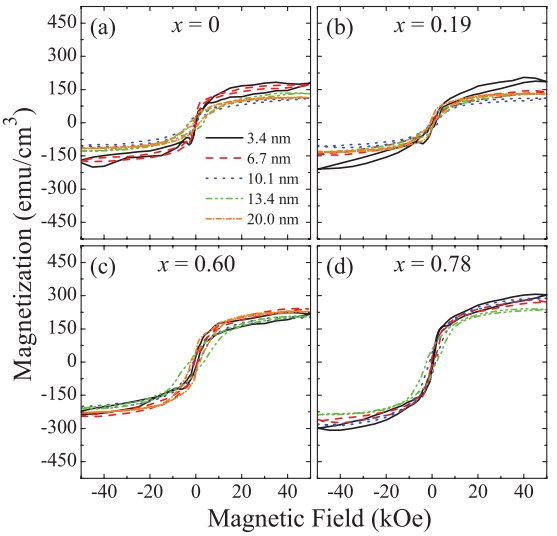

FIG. 3. (Color online) Out-of-plane M-H loops at 300 K of $Co_{1-x}Fe_{2+x}O_4$ films with stoichiometries of (a) $x = 0$, (b) $x = 0.19$, (c) $x = 0.60$, and (d) $x = 0.78$.

B. Cation distribution

XAS measurements were carried out to determine if the cation distribution for $Co_{1-x}Fe_{2+x}O_4$ thin films changes as the film thickness is reduced. It has been previously proposed that a decrease in the inversion parameter is the cause for the enhanced magnetic moments observed in ultrathin spinel ferrites.[7,8] Previous studies on Fe-doped $CoFe_2O_4$ demonstrated that the inversion parameter can be determined through comparison of XAS measurements with ligand field multiplet (LFM) calculations.[20,40,41] These studies concluded that the Fe^{2+} cations in $Co_{1-x}Fe_{2+x}O_4$ occupy octahedral sites only, while the Co^{2+} cations occupy both octahedral and tetrahedral sties. This results in the cobalt cation distribution being solely responsible for the inversion parameter of the crystal structure. Figure 4(a) displays the Co $L_{2,3}$ XAS measurements for $Co_{0.40}Fe_{2.60}O_4$ films with thicknesses ranging from 3.4 to 20.0 nm; Fig. 4(b) shows the L_3 edge in greater detail (spectra for other $Co_{1-x}Fe_{2+x}O_4$ samples are similar). The L_3edge is characterized by three peaks at 776.3, 777.7, and 778.8 eV, while the L_2 edge only contains one fairly broad peak around 793.1 eV. The spectra for the different thickness $Co_{0.40}Fe_{2.60}O_4$ films are nearly identical to each other, indicating that there is little difference in the cation distribution between these five films.

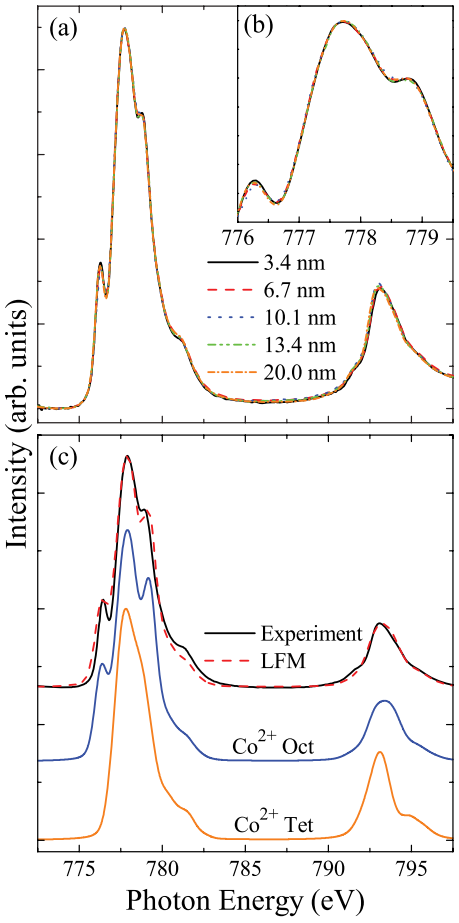

FIG. 4. (Color online) (a) Experimental Co $L_{2,3}$ XAS spectra for $Co_{0.40}Fe_{2.60}O_4$ thin films with thicknesses of 3.4, 6.7, 10.1, 13.4, and 20.0 nm (similar XAS spectra are seen for other $Co_{1-x}Fe_{2+x}O_4$ samples). (b) L_3 edge for the spectra in (a). (c) Comparison of the Co $L_{2,3}$ XAS experimental and LFM-calculated spectra for 20.0 nm $Co_{0.40}Fe_{2.60}O_4$ sample; shown below are the individual LFM spectra for Co^{2+} octahedral and tetrahedral cations.

LFM calculations were performed using the program CTM4XAS[42] to quantitatively determine the inversion parameter of each film. Theoretical spectra for the Co^{2+} octahedral and tetrahedral cations were calculated and summed in a weighted, linear superposition to produce a theoretical spectrum for each film; this spectrum was compared to the experimental spectrum to determine the Co^{2+} octahedral/tetrahedral cation ratio and the inversion parameter. The individual cation LFM spectra, along with the LFM and experimental 20.0 nm $Co_{0.40}Fe_{2.60}O_4$ spectra, are shown in Fig. 4(c). The LFM calculations were made with the $2p$ and $3d$ spin-orbit interactions reduced to 99% and 75% of their bulk values, respectively; the $F(dd)$, $F(pd)$, and $G(pd)$ Slater integrals reduced to 70%, 80%, and 75% of their Hartree-Fock values, respectively; and crystal fields of 1.2 and 0.6 eV for the octahedral and tetrahedral cations, respectively. The spectra were broadened by a Lorentzian with a half-width of 0.1 (0.3) eV for the L_3 (L_2) edge and by a Gaussian with a half-width of 0.34 eV. These parameters were chosen by visually fitting the calculated spectra to the experimental spectra and are consistent with previous calculations of Fe_3O_4 and $CoFe_2O_4$ thin films.[43–45] A comparison of the Co^{2+} octahedral and tetrahedral LFM spectra clearly shows that Co^{2+} cations located in different symmetry sites have different line shapes and contribute intensity to different peaks in the L_3 edge, with the octahedral cations contributing intensity to all three L_3 peaks and the tetrahedral cations contributing intensity to only the central L_3 peak.

The inversion parameter for each sample, as determined from the XAS experiments and LFM calculations, is shown in Fig. 5; a linear fit is provided for each sample set as a guide to the eye. It is clear from this figure that the inversion parameter does not change systematically as the film thickness is reduced;

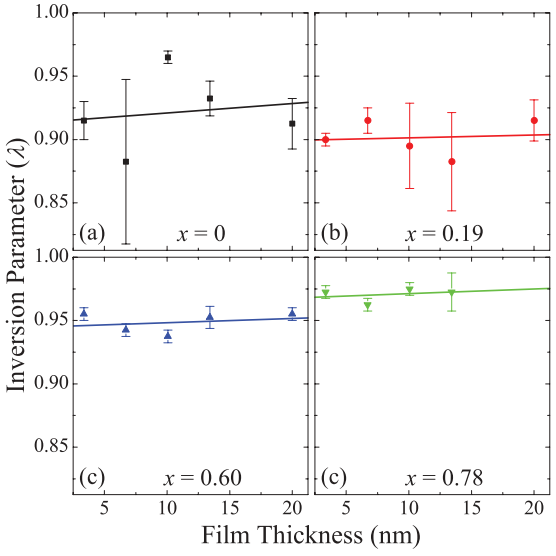

FIG. 5. (Color online) Inversion parameter vs film thickness for $Co_{1-x}Fe_{2+x}O_4$ films with stoichiometries of (a) $x = 0$, (b) $x = 0.19$, (c) $x = 0.60$, and (d) $x = 0.78$. Linear fits to the data provide a guide to the eye.

instead it seems to change randomly. The best fit lines do show that the inversion parameter tends to decrease slightly for all $Co_{1-x}Fe_{2+x}O_4$ stoichiometries as the film thickness is reduced; however, the amount of decrease is quite small for all stoichiometries, on the order of 1%. Since the inversion parameter does not change systematically and only has a very slight tendency to decrease as the film thickness is reduced, it can be concluded that a change in cation distribution is not responsible for the enhanced magnetic moment measured in these ultrathin Fe-doped $CoFe_2O_4$ films.

C. X-ray magnetic linear dichroism

XMLD measurements, which are dependent on $\langle M^2 \rangle$ of the cations,[46] have been utilized to gain information about the magnetic properties of the individual cations. The measurements were performed with the samples in an out-of-plane remanent magnetization state, and the x-ray absorption was measured for angles of 30°, 45°, 60°, 75°, and 90° between the $\boldsymbol{E}$ field of the x rays and the [001] crystal direction for the 20.0 nm samples, and angles of 30° and 90° for the other samples. The x-ray absorption scans were normalized to the Fe doping level so that spectra of the same sample in each orientation have the same integrated intensity. This allowed for a qualitative analysis of the relative changes in the XMLD spectra, while minimizing any effects due to the changing angle of incidence between the $\boldsymbol{E}$ field of the x rays and the surface normal (i.e., saturation effects). The angle-dependent measurements were used to interpolate the spectra with the $\boldsymbol{E}$ field of the x rays parallel ($I_\parallel$) and perpendicular ($I_\perp$) to the surface normal using the angle-dependent XMLD equation[47]

$$I(\theta) = I_\parallel \cos^2\theta + I_\perp \sin^2\theta. \quad (1)$$

Figure 6(a) displays the Co $L_{2,3}$ $I_\parallel$, $I_\perp$, and XMLD spectra for the 20.0 nm $Co_{0.40}Fe_{2.60}O_4$ film, while Figs. 6(b)–6(e) show the XMLD spectra for $Co_{1-x}Fe_{2+x}O_4$ films with Fe doping levels of $x = 0$, 0.19, 0.60, and 0.78, respectively, and film thicknesses ranging from 3.4 to 20.0 nm. The spectra are characterized by a negative peak at 776.3 eV and two positive peaks at 777.2 and 778.3 eV in the L_3 edge, and a large positive peak at 792.9 and a small negative peak at 794.4 eV in the L_2 edge. XMLD of ultrathin films can be difficult to measure owing to large amounts of noise; however, a general trend appears among each of the sample sets, in which the linear dichroism decreases as the film thickness is reduced. A previous study of the 20.0 nm Fe-doped $CoFe_2O_4$ films, which modeled the spectra with LFM calculations, determined that the main cause of the dichroism in these samples is an aligned magnetic spin axis, not anisotropic bonding caused by film strain.[18] Hence, the decrease in dichroism that is seen as the film thickness is reduced is evidence that the magnetic spin axis of the Co^{2+} cations is becoming, on average, more canted away from the [001] crystal direction.

The Fe $L_{2,3}$ $I_\parallel$, $I_\perp$, and XMLD spectra for the 20.0 nm $Co_{0.40}Fe_{2.60}O_4$ film are displayed in Fig. 7(a), with the XMLD spectra for all the $Co_{1-x}Fe_{2+x}O_4$ samples shown in Figs. 7(b)–7(e). These XMLD spectra are characterized in the L_3 region by negative peaks at 706, 707.5, and 710.2 eV and positive peaks at 706.7 and 708.8 eV; and in the L_2 region by negative peaks at 718.7 and 720.5 eV and positive peaks at

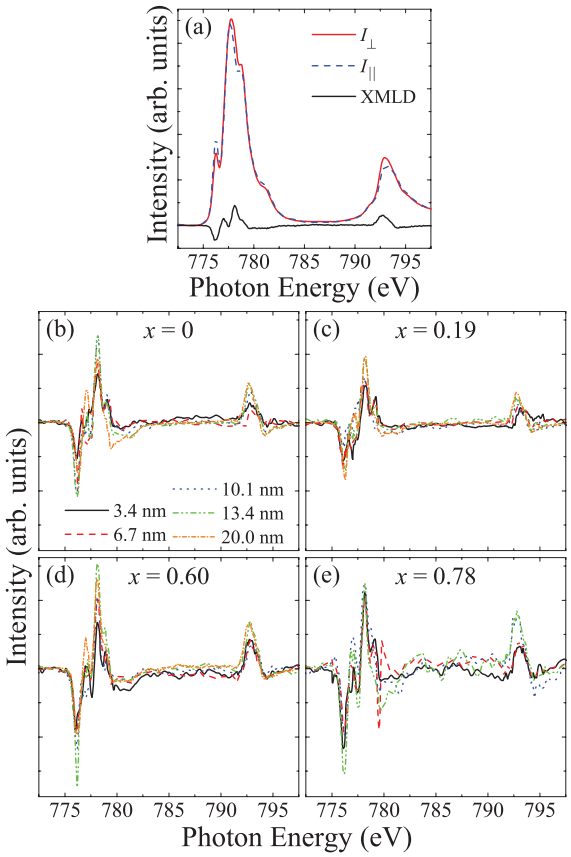

FIG. 6. (Color online) (a) Interpolated Co $L_{2,3}$ XAS spectra for a 20.0 nm $Co_{0.40}Fe_{2.60}O_4$ film with the electric field of the x-rays polarized perpendicular and parallel to the [001] crystal direction, and the corresponding XMLD spectrum. Co $L_{2,3}$ XMLD spectra for $Co_{1-x}Fe_{2+x}O_4$ films with stoichiometries of (b) $x = 0$, (c) $x = 0.19$, (d) $x = 0.60$, and (e) $x = 0.78$.

719.8 and 722.3 eV. Previous LFM modeling of these spectra also concluded that the majority of the dichroism originates from the alignment of the magnetic spin axes.[18] In addition, the modeling determined that certain types of cations only contributed intensity to certain peaks; in particular, the Fe^{2+} cations only contribute intensity to the three negative L_3 peaks and the two low energy L_2 peaks. As the film thickness is reduced, none of the peaks remains at a constant intensity, and the large majority of the peaks have a maximum intensity for one of the two thickest films (13.4 or 20.0 nm). Since specific peaks are associated with certain types of cations, and the majority of the peaks are decreasing with decreasing film thickness, we conclude that all types of cations have magnetic spin axes that are becoming less aligned with the [001] crystal direction as the film thickness is reduced.

IV. DISCUSSION

The results presented above provide a better understanding of the physical nature of the enhanced magnetic moment in ultrathin Fe-doped $CoFe_2O_4$ thin films. Of the two potential sources for this enhanced magnetization that have previously been proposed, a transition to a superparamagnetic state that has been observed in Fe_3O_4 and a change in cation distribution

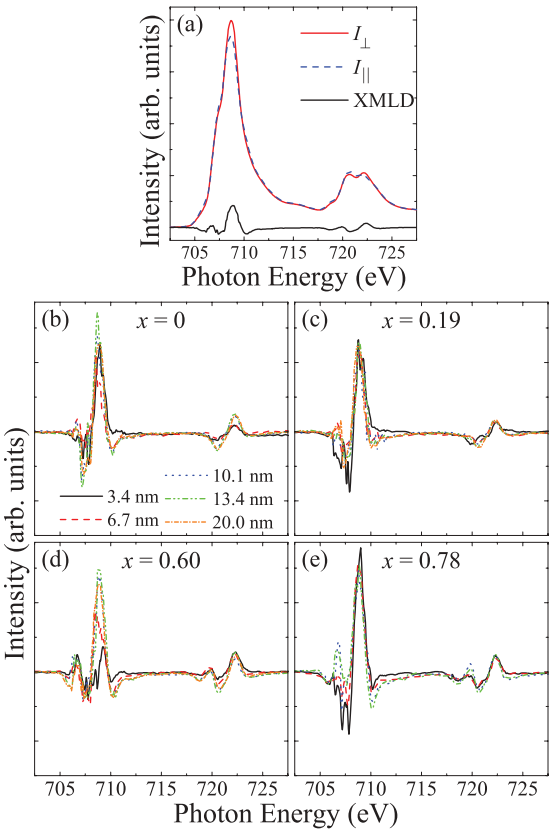

FIG. 7. (Color online) (a) Interpolated Fe $L_{2,3}$ XAS spectra for a 20.0 nm $Co_{0.40}Fe_{2.60}O_4$ film with the electric field of the x-rays polarized perpendicular and parallel to the [001] crystal direction, and the corresponding XMLD spectrum. Fe $L_{2,3}$ XMLD spectra for $Co_{1-x}Fe_{2+x}O_4$ films with stoichiometries of (b) $x = 0$, (c) $x = 0.19$, (d) $x = 0.60$, and (e) $x = 0.78$.

that has been suggested for $CoFe_2O_4$ and $NiFe_2O_4$, the results clearly eliminate a change in cation distribution as the cause of the enhanced magnetic moment. This is concluded from the XAS measurements and LFM calculations, which show that there is no large change in the cation distribution with a reduction in film thickness. This leaves superparamagnetism as the potential source of this enhanced magnetic moment.

Superparamagnetism is a magnetic state that occurs in materials that are small enough that the thermal energy can overcome the magnetic anisotropy energy of the system, resulting in thermally activated, random fluctuations of the magnetic spins.[48,49] Evidence for a transition to a superparamagnetic state upon a reduction in film thickness is seen in both the SQUID and XMLD measurements. The coercive fields and remanent magnetic moments are strongly reduced in these films as the film thickness is reduced and nearly vanish for the thinnest films (3.4 and 6.7 nm) at room temperature, evidence of a sharp reduction in the magnetic anisotropy for these thinnest films. More direct evidence for a superparamagnetic state is seen in the XMLD measurements, where a decrease in the film thickness is accompanied by a decrease of the spin alignment with the [001] crystal direction for all of the cations. Since XMLD measures the average spin direction, this decrease in the alignment of the spins can also be interpreted as an increase in the fluctuations of the spins, and hence evidence for a superparamagnetic state. In order to have a superparamagnetic state in the spinel ferrites, the presence of antiphase boundaries is necessary since each crystallographic domain can be a single magnetic domain and act independently as an individual superparamagnet.[6] It is also well known that density of antiphase boundaries increases as the film thickness is decreased[50] and that large densities of antiphase boundaries result in thin-film ferrites having reduced magnetic moments.[18,29] Therefore, it has been previously proposed for ultrathin Fe_3O_4/MgO[6] that the enhanced magnetic moment is a result of the effect of antiphase boundaries on the magnetic moment being weakened in the superparamagnetic state; this interpretation seems to fit the data presented here as well.

If the antiphase boundaries are what drive ultrathin ferrites into a superparamagnetic state, then it is important to consider the substrates used for growth when comparing different studies. Whereas the substrate used in this work and for the previous work on Fe_3O_4[6] was MgO, the substrate used in the prior studies of $CoFe_2O_4$[7] and $NiFe_2O_4$,[8] which suggested that changes in cation distribution were the source of an enhanced magnetic moments, was $SrTiO_3$. Recent work on Fe-doped $CoFe_2O_4$ on $SrTiO_3$ suggests that there is an elimination of the antiphase boundaries and/or that they have a reduced effect on the magnetic moment.[51] If antiphase boundaries are eliminated in ferrite films grown on $SrTiO_3$, then the enhanced magnetic moment in these films may in fact be partially due to cation distribution changes. These changes could be caused by the large lattice mismatch between spinel ferrites and $SrTiO_3$ ($\sim$7%) or due to the growth method (pulsed laser deposition or sputtering may produce films that are more disordered than those grown by MBE).[52] However, given the direct evidence of a phase transition to a superparamagnetic state in this work and the previous work on Fe_3O_4,[6] it is necessary to always consider the role that superparamagnetism might play in the enhanced magnetic moment of ultrathin spinel ferrites grown on any substrate. This analysis shows that determining the exact origin of the enhanced magnetic moment in ultrathin ferrites is challenging and may include additional factors such as substrate and growth method.

V. CONCLUSIONS

In summary, the effect of film thickness on the magnetic properties of $Co_{1-x}Fe_{2+x}O_4$ ($0 \leqslant x \leqslant 0.78$) has been investigated by use of SQUID magnetometry and XMLD for ultrathin films grown on MgO (001) by oxide-MBE for thicknesses ranging between 3.4 and 20 nm. These measurements concluded that the magnetic moment increases as the film thickness is reduced for all Fe doping levels; however, this increase in magnetic moment is accompanied by a decrease in the coercive fields, remanent magnetic moments and alignment of the spin axes of all of the cations with the [001] crystal direction. The cation distribution was explicitly measured for the first time by use of XAS experiments and LFM calculations, and it was found that there is no significant change in the inversion parameter as the film thickness is reduced, eliminating this hypothesis as the potential reason for the enhancement of the magnetic moments. However, the results of the SQUID and XMLD measurements are consistent

with the films consisting of magnetically independent small domains confined by antiphase boundaries, which are also responsible for the onset of a superparamagnetic state at room temperature, as has been shown for ultrathin Fe_3O_4/MgO films.[6] The weakened effect of the antiphase boundaries on pinning the sublattice magnetizations results in an enhanced magnetic moment in ultrathin films. The increase in the magnetic moment upon a reduction of film thickness, and the possible existence of a phase transition from a ferrimagnetic to a superparamagnetic state must be taken into account when incorporating ultrathin ferrite films in spintronic applications, such as spin filters and magnetic tunnel junctions, and the interpretation of the results of these devices.

ACKNOWLEDGMENTS

The authors acknowledge primary financial support by the NSF through MRSEC DMR 1119826 (CRISP). Use of the National Synchrotron Light Source, Brookhaven National Laboratory, was supported by the US Department of Energy, Office of Science, Office of Basic Energy Sciences, under Contract No. DE-AC02-98CH10886.

*Present address: Department of Physics, Pennsylvania State University, University Park, PA 16802, USA.

[1] J. Cibert, J. F. Bobo, and U. Luders, C. R. Phys. **6**, 977 (2005).
[2] S. A. Wolf, D. D. Awschalom, R. A. Buhrman, J. M. Daughton, S. von Molnar, M. L. Roukes, A. Y. Chtchelkanova, and D. M. Treger, Science **294**, 1488 (2001).
[3] I. Zutic, J. Fabian, and S. Das Sarma, Rev. Mod. Phys. **76**, 323 (2004).
[4] G. F. Dionne, *Magnetic Oxides* (Springer Science + Business Media, Boston, 2009).
[5] M. Huijben, L. W. Martin, Y. H. Chu, M. B. Holcomb, P. Yu, G. Rijnders, D. H. A. Blank, and R. Ramesh, Phys. Rev. B **78**, 094413 (2008).
[6] F. C. Voogt, T. T. M. Palstra, L. Niesen, O. C. Rogojanu, M. A. James, and T. Hibma, Phys. Rev. B **57**, R8107 (1998).
[7] F. Rigato, J. Geshev, V. Skumryev, and J. Fontcuberta, J. Appl. Phys. **106**, 113924 (2009).
[8] U. Luders, M. Bibes, J. F. Bobo, M. Cantoni, R. Bertacco, and J. Fontcuberta, Phys. Rev. B **71**, 134419 (2005).
[9] Z. Szotek, W. M. Temmerman, D. Kodderitzsch, A. Svane, L. Petit, and H. Winter, Phys. Rev. B **74**, 174431 (2006).
[10] V. N. Antonov, B. N. Harmon, and A. N. Yaresko, Phys. Rev. B **67**, 024417 (2003).
[11] H.-T. Jeng and G. Y. Guo, J. Magn. Magn. Mater. **239**, 88 (2002).
[12] M. Penicaud, B. Siberchicot, C. B. Sommers, and J. Kubler, J. Magn. Magn. Mater. **103**, 212 (1992).
[13] P. I. Slick, in *Ferromagnetic Materials: A Handbook on the Properties of Magnetically Ordered Substances*, edited by E. P. Wohlfarth, Vol. 2 (North-Holland, Amsterdam, Netherlands, 1980), p. 189.
[14] G. Hu and Y. Suzuki, Phys. Rev. Lett. **89**, 276601 (2002).
[15] A. V. Ramos, M. J. Guittet, J. B. Moussy, R. Mattana, C. Deranlot, F. Petroff, and C. Gatel, Appl. Phys. Lett. **91**, 122107 (2007).
[16] U. Luders, M. Bibes, K. Bouzehouane, E. Jacquet, J. P. Contour, S. Fusil, J. F. Bobo, J. Fontcuberta, A. Barthelemy, and A. Fert, Appl. Phys. Lett. **88**, 082505 (2006).
[17] H. Zheng, J. Wang, S. E. Lofland, Z. Ma, L. Mohaddes-Ardabili, T. Zhao, L. Salamanca-Riba, S. R. Shinde, S. B. Ogale, F. Bai, D. Viehland, Y. Jia, D. G. Schlom, M. Wuttig, A. Roytburd, and R. Ramesh, Science **303**, 661 (2004).
[18] J. A. Moyer, C. A. F. Vaz, D. A. Arena, D. Kumah, E. Negusse, and V. E. Henrich, Phys. Rev. B **84**, 054447 (2011).
[19] D. Venkateshvaran, M. Althammer, A. Nielsen, S. Geprags, M. S. Ramachandra Rao, S. T. B. Goennenwein, M. Opel, and R. Gross, Phys. Rev. B **79**, 134405 (2009).
[20] J. A. Moyer, C. A. F. Vaz, E. Negusse, D. A. Arena, and V. E. Henrich, Phys. Rev. B **83**, 035121 (2011).
[21] J. Takaobushi, H. Tanaka, T. Kawai, S. Ueda, J.-J. Kim, M. Kobata, E. Ikenaga, M. Yabashi, K. Kobayashi, Y. Nishino, D. Miwa, K. Tamasaku, and T. Ishikawa, Appl. Phys. Lett. **89**, 242507 (2006).
[22] J. Takaobushi, M. Ishikawa, S. Ueda, E. Ikenaga, J.-J. Kim, M. Kobata, Y. Takeda, Y. Saitoh, M. Yabashi, Y. Nishino, D. Miwa, K. Tamasaku, T. Ishikawa, I. Satoh, H. Tanaka, K. Kobayashi, and T. Kawai, Phys. Rev. B **76**, 205108 (2007).
[23] G. A. Sawatzky, F. van der Woude, and A. H. Morrish, Phys. Rev. **187**, 747 (1969).
[24] G. Hu, J. H. Choi, C. B. Eom, V. G. Harris, and Y. Suzuki, Phys. Rev. B **62**, R779 (2000).
[25] J. A. Moyer, D. Kumah, C. A. F. Vaz, D. A. Arena, and V. E. Henrich, Appl. Phys. Lett. **101**, 021907 (2012).
[26] S. A. Chambers, R. F. C. Farrow, S. Maat, M. F. Toney, L. Folks, J. G. Catalano, T. P. Trainor, and G. E. Brown, Jr., J. Magn. Magn. Mater. **246**, 124 (2002).
[27] Y. Suzuki, G. Hu, R. B. van Dover, and R. J. Cava, J. Magn. Magn. Mater. **191**, 1 (1999).
[28] G. Hu, V. G. Harris, and Y. Suzuki, IEEE Trans. Magn. **37**, 2347 (2001).
[29] D. T. Margulies, F. T. Parker, M. L. Rudee, F. E. Spada, J. N. Chapman, P. R. Aitchison, and A. E. Berkowitz, Phys. Rev. Lett. **79**, 5162 (1997).
[30] M. Tachiki, Prog. Theor. Phys. **23**, 1055 (1960).
[31] J. C. Slonczewski, Phys. Rev. **110**, 1341 (1958).
[32] J. C. Slonczewski, J. Appl. Phys. **29**, 448 (1958).
[33] L. Horng, G. Chern, M. C. Chen, P. C. Kang, and D. S. Lee, J. Magn. Magn. Mater. **270**, 389 (2004).
[34] R. V. Chopdekar and Y. Suzuki, Appl. Phys. Lett. **89**, 182506 (2006).
[35] A. V. Ramos, T. S. Santos, G. X. Miao, M. J. Guittet, J. B. Moussy, and J. S. Moodera, Phys. Rev. B **78**, 180402(R) (2008).
[36] F. Zavaliche, H. Zheng, L. Mohaddes-Ardabili, S. Y. Yang, Q. Zhan, P. Shafer, E. Reilly, R. Chopdekar, Y. Jia, P. Wright, D. G. Schlom, Y. Suzuki, and R. Ramesh, Nano Lett. **5**, 1793 (2005).
[37] Y. Zhang, C. Y. Deng, J. Ma, Y. H. Lin, and C. W. Nan, Appl. Phys. Lett. **92**, 062911 (2008).
[38] J. H. Park, J.-H. Lee, M. G. Kim, Y. K. Jeong, M.-A. Oak, H. M. Jang, H. J. Choi, and J. F. Scott, Phys. Rev. B **81**, 134401 (2010).
[39] C. A. F. Vaz, J. Hoffman, C. H. Anh, and R. Ramesh, Adv. Mater. **22**, 2900 (2010).
[40] F. M. F. de Groot, J. C. Fuggle, B. T. Thole, and G. A. Sawatzky, Phys. Rev. B **42**, 5459 (1990).

[41]G. van der Laan and I. W. Kirkman, J. Phys.: Condens. Matter **4**, 4189 (1992).
[42]E. Stavitski and F. M. F. de Groot, Micron **41**, 687 (2010).
[43]P. Kuiper, B. G. Searle, L.-C. Duda, R. M. Wolf, and P. J. van der Zaag, J. Electron Spectrosc. Relat. Phenom. **86**, 107 (1997).
[44]E. Arenholz, G. van der Laan, R. V. Chopdekar, and Y. Suzuki, Phys. Rev. B **74**, 094407 (2006).
[45]G. van der Laan, E. Arenholz, R. V. Chopdekar, and Y. Suzuki, Phys. Rev. B **77**, 064407 (2008).
[46]B. T. Thole, G. Vanderlaan, and G. A. Sawatzky, Phys. Rev. Lett. **55**, 2086 (1985).
[47]J. Stohr and H. C. Siegmann, *Magnetism: From Fundamentals to Nanoscale Dynamics* (Springer, Berlin, 2006).
[48]J. L. Dormann, D. Fiorani, and E. Tronc, Adv. Chem. Phys. **98**, 283 (1997).
[49]C. A. F. Vaz, J. A. C. Bland, and G. Lauhoff, Rep. Prog. Phys. **71**, 056501 (2008).
[50]W. Eerenstein, T. T. M. Palstra, T. Hibma, and S. Celotto, Phys. Rev. B **66**, 201101R (2002).
[51]J. A. Moyer, C. A. F. Vaz, D. P. Kumah, D. A. Arena, and V. E. Henrich (unpublished).
[52]W. A. Doolittle, A. G. Carver, and W. Henderson, J. Vac. Sci. Technol. B **23**, 1272 (2005).